

# 莫桑比克太特省钛铁矿田斜长岩锆石 U-Pb 年龄、地球化学特征及成矿、大地构造意义

刘高峰<sup>1)</sup>, 楼法生<sup>1)</sup>, 罗春林<sup>1)</sup>, 王斌<sup>1)</sup>, 廖六根<sup>1)</sup>, 卢先锋<sup>1)</sup>, 陈浩鹏<sup>1)</sup>,  
朱昌杰<sup>1)</sup>, CUMBANE Antonio<sup>2)</sup>, 刘永旭<sup>3)</sup>

1) 江西省地质调查研究院, 南昌, 330030, 中国; 2) 马多拉省地质矿产能源局, 马多拉, 1115, 莫桑比克;  
3) 江西省煤田地质勘察研究院, 南昌, 330030, 中国

**内容提要:**莫桑比克位于南部非洲, 矿产资源极其丰富, 是钛矿主要出口大国, 目前主要开发利用的以海岸沿线的钛锆沙矿为主, 钛铁矿原生矿的开发利用及其成矿地质背景研究程度相对较低。本文采集了莫桑比克太特省一带与原生钛铁矿共生的斜长岩系列分析样品, 对斜长岩样品锆石 U-Pb 定年, 获得岩石形成的地质年龄为  $580 \pm 5$  Ma; 样品岩石化学特征反映了斜长岩属低 Ti、低 Mg、低 K 拉斑玄武岩系列; 稀土地球化学元素反映斜长石堆积明显,  $\delta\text{Eu}$  出现极高的正异常; LREE/HREE 比值为  $8.27 \sim 21.44$ , 总体显示为轻稀土富集型稀土配分模式曲线, 指示了斜长岩为深部原始地幔高度熔融及结晶分异而成; 微量元素中具有明显的富集 Rb、Sr、Ba 等大离子亲石元素, 亏损 Zr、Nb 等高场强元素, 并且 Ta/Hf 比值为  $0.1 \sim 0.26$ , Th/Ta 比值为  $3.14 \sim 13.59$ , 反映斜长岩形成于陆内弧后伸展构造环境。通过对钛铁矿成矿围岩的研究, 揭示了钛铁矿的成因类型为岩浆晚期结晶分异型, 成矿模式为结晶分异压滤型; 同时揭露了莫桑比克赞比亚构造带  $660 \sim 610$  Ma 泛非造山运动重要证据。

**关键词:**莫桑比克太特省; 钛铁矿; 斜长岩; 地球化学; 成矿; 大地构造意义

莫桑比克属南部非洲地块, 从太古宙克拉通 (Archaean craton) 到中—新元古代罗地尼亚 (Rodinia) 超大陆, 再到新元古代—早古生代冈瓦纳 (Gondwana) 古大陆, 经历了相对较长时间复杂的拉张—汇聚—拼接—造山等板块运动。总体而言, 莫桑比克所属南部非洲板块, 主要有三个时期的造山事件: 古元古代造山事件  $2.05 \sim 1.8$  Ga, 中元古代造山事件  $1.35 \sim 1.0$  Ga, 新元古代—早古生代泛非造山事件  $800 \sim 410$  Ma (Marco, 1984; Brito Neves et al., 1999; Kröner, 2001; Hanson, 2003; Huang Jianping et al., 2015; Liu Xiaoyang et al., 2005, 2017; Ren Junping et al., 2019; Gu Alei et al., 2020)。古元古代造山事件, 在南部非洲主要表现坦桑尼亚太古宙克拉通南部的 Ubendian 构造带和 Usagaran 构造带, 以及津巴布韦太古宙克拉通西北部的 Magondi

构造带 (Costa M et al., 1992; Zuo Libo et al., 2020); 在莫桑比克境内则为津巴布韦太古宙克拉通、南非 Kaapvaal 克拉通之间的 Linpopo 构造带。中元古代造山事件标志着 Rodinia 古大陆的拼接过程, 在南部非洲主要表现为赞比亚东侧 Irumide 构造带、坦桑尼亚西侧的 Kibaran 构造带 (Sacchi et al., 2000; Haslam et al., 1983; Hanson et al., 1998)。新元古代—早古生代泛非造山事件, 在南部非洲主要表现为纳米比亚 Damara 构造带、赞比亚 Lufilian 弧以及坦桑尼亚东侧的莫桑比克构造带 (Pinna et al., 1993; Maboko, 1995; De Wit et al., 2001; Gu Alei et al., 2020)。莫桑比克赞比亚构造带和莫桑比克构造带同时叠加了中元古代造山事件和新元古代—早古生代造山事件 (Andreoli et al., 1984; Evans et al., 1999; Jamal et al., 1999;

注: 本文为 2010 年国外风险勘查资金项目资助的成果 (编号: 10141014B011)。

收稿日期: 2020-06-24; 改回日期: 2020-08-03; 网络发表日期: 2020-11-17; 责任编辑: 黄敏。

作者简介: 刘高峰, 男, 1986 年, 高级工程师, 硕士, 长期从事区域地质矿产调查与研究, Email: oasiskobe@163.com

**引用本文:** 刘高峰, 楼法生, 罗春林, 王斌, 廖六根, 卢先锋, 陈浩鹏, 朱昌杰, CUMBANE Antonio, 刘永旭. 2021. 莫桑比克太特省钛铁矿田斜长岩锆石 U-Pb 年龄、地球化学特征及成矿、大地构造意义. 地质学报, 地质学报, 95(4): 1100~1113, doi: 10.19762/j.cnki.dizhixuebao.2021017.

Liu Gaofeng, Lou Fasheng, Luo Qunlin, Wang Bin, Liao Liugen, Lu Xianfeng, Chen Haopeng, Zhu Changjie, Cumbane Antonio, Liu Yongxu. 2021. Zircon U-Pb age, geochemical characteristics and mineralization, geotectonic significance for anorthosite of the ilmenite field in Tete Province, Mozambique. Acta Geologica Sinica, 95(4): 1100~1113.

Grantham et al., 2003)。

泛非构造运动标志着冈瓦纳古大陆的拼接,较新元古代之前的构造运动,该构造事件具有复杂、多阶段性特点(Dalziel, 1994; Anne Grunow et al., 1996; Frimmel et al., 2001; Bingen et al., 2009)。有学者认为泛非造山运动为 760~730Ma (Stern, 1994; Handke et al., 1999; Tucker et al., 1999; Kröner et al., 2000; Key et al., 2001; Meert, 2003; Collins et al., 2005; Johnson et al., 2006; Ashwal et al., 2007; Bingen et al., 2009; Bjerkögörd et al., 2009)、660~610Ma (Ashwal et al., 1998; Jacobs et al., 1998; Kröner et al., 2001; Johnson et al., 2006)、570~530Ma (Johnson et al., 2003, 2005, 2007; Gray et al., 2008; Viola et al., 2008; Jacobs et al., 2008; Bingen et al., 2009; Beaumont et al., 2009; Macey et al., 2010)三个阶段;也有学者认为泛非造山运动为 575~545Ma、545~530Ma、530~500Ma (Anne Grunow et al., 1996; Hauzenberger et al., 2004, 2007; Cutten et al., 2006)三个阶段。研究区所属赞比西构造带是一个长时间连续的造山地块 (Goscombe et al., 2000; Kröner et al., 2000; Hanson, 2003),但也有学者认为造山运动并非长时间连续过程,区内所见中元古代地块为泛非造山运动携带的飞来峰 (Kröner, 2001)。对于斜长岩型钛铁矿,国内外已经有学者对全球典型矿山进行了较多的相关研究工作 (Wilmart et al., 1989; Hu Shiling et al., 1990; Druppel et al., 2001; Duchesne, 1999; Diot et al., 2003; Charlier et al., 2006, 2015; Zhang Lianfeng et al., 2006; Chen Zhengle et al., 2014; Chen Terry Wei et al., 2016; Zhou Yonggang, 2019),但不同区域矿山成因类型以及成矿机制各不相同。也有学者对莫桑比克钛铁砂矿与原生矿做了系列研究工作,但研究程度不深 (Evans et al., 1999; He Heling et al., 2012; Zhang Jianwen et al., 2013; Xiao Xiaolin et al., 2014; Deng Yutao et al., 2017; Fu Li, 2019)。

本文旨在通过对莫桑比克太特省钛铁矿围岩斜长岩 LA-ICP-MS 锆石 U-Pb 年代学、地球化学等方面的研究,确定该区与钛铁矿成矿相关围岩的地质年龄,探讨研究区斜长岩成因、钛铁矿的成因模式、地质构造环境,并对区内新元古代—早古生代岩浆构造演化提供约束;并综合对比相似矿床,为下一步区内钛铁矿找矿提供理论依据。

## 1 地质背景

莫桑比克境内可分为 4 个构造地块(层)(图 1a):①太古宙—古元古代津巴布韦-马尼卡克拉通,分布于莫桑比克中部与津巴布韦邻近;②同时包括中元古代造山事件与新元古代—早古生代泛非造山运动事件的莫桑比克构造带 (MoZB),分布于莫桑比克北东部,与坦桑尼亚接壤以北主体为泛非构造带;③同时包括中元古代造山事件与新元古代—早古生代泛非赞比西构造带 (ZB),主要分布于莫桑比克西北部,以赞比西河为界,南部多为泛非构造带;④显生宙中新生代覆盖层,主要分布于莫桑比克内部盆地以及东部滨印度洋渐变带。

太特省位于莫桑比克的西北部,属于赞比西构造带 (ZB) 范畴。太特省主要发育古元古代—新元古代地质体,南部(赞比西河以南)为显生宙覆盖层(图 1b)。区内古元古代鲁辛噶 (Rushinga) 岩群、希度尔 (Chidue) 岩群,岩性为黑云石英斜长片麻岩、黑云母片麻岩等副片麻岩以及大量的大理岩。区内中元古代地质体出露相对较广,变质岩层以赞布尔 (Zambue) 岩群、巴鲁尔 (Barue) 岩群、安格尼亚 (Angonia) 岩群、鲁依阿 (Luia) 岩群、芬格 (Fingoe) 岩群为主,岩性为浅色片麻岩、长英质片麻岩、石榴黑云斜长片麻岩、铁镁质麻粒岩等;变质岩体以芬格 (Fingoe) 花岗岩、德萨朗哈马 (Desaranhama) 花岗岩、辛达 (Sinda) 花岗岩为主,主要岩性为片麻状花岗岩、片麻状正长花岗岩以及片麻状二长花岗岩。区内新元古代—早古生代斜长岩甚为发育,同时也可见有大量的钛铁矿层,本次研究对象为与安格尼亚岩群呈侵入接触关系的斜长岩。

本次在研究区测得斜长岩与钛铁矿实测剖面 Pm1 (图 2),剖面中可见有中元古代安格尼亚群 3 个岩组,岩性分别为浅灰色—灰色中粒石榴黑云角闪斜长片麻岩、灰色中粒黑云角闪斜长片麻岩、浅灰色中粒黑云斜长片麻岩。斜长岩与安格尼亚群呈侵入接触关系,与钛铁矿之间呈共生突变-渐变接触关系。

## 2 岩石学、岩相学特征

斜长岩在区内主要为岩滴状、岩枝状产出,与围岩之间呈侵入接触关系、与钛铁矿之间呈突变-渐变过渡关系(图 3a, 3b)。岩石呈浅灰白色—浅灰黄色,中粗粒结构,块状构造。本次研究在剖面和钻孔中采集斜长岩薄片鉴定样品 5 件(同化学全分析样),

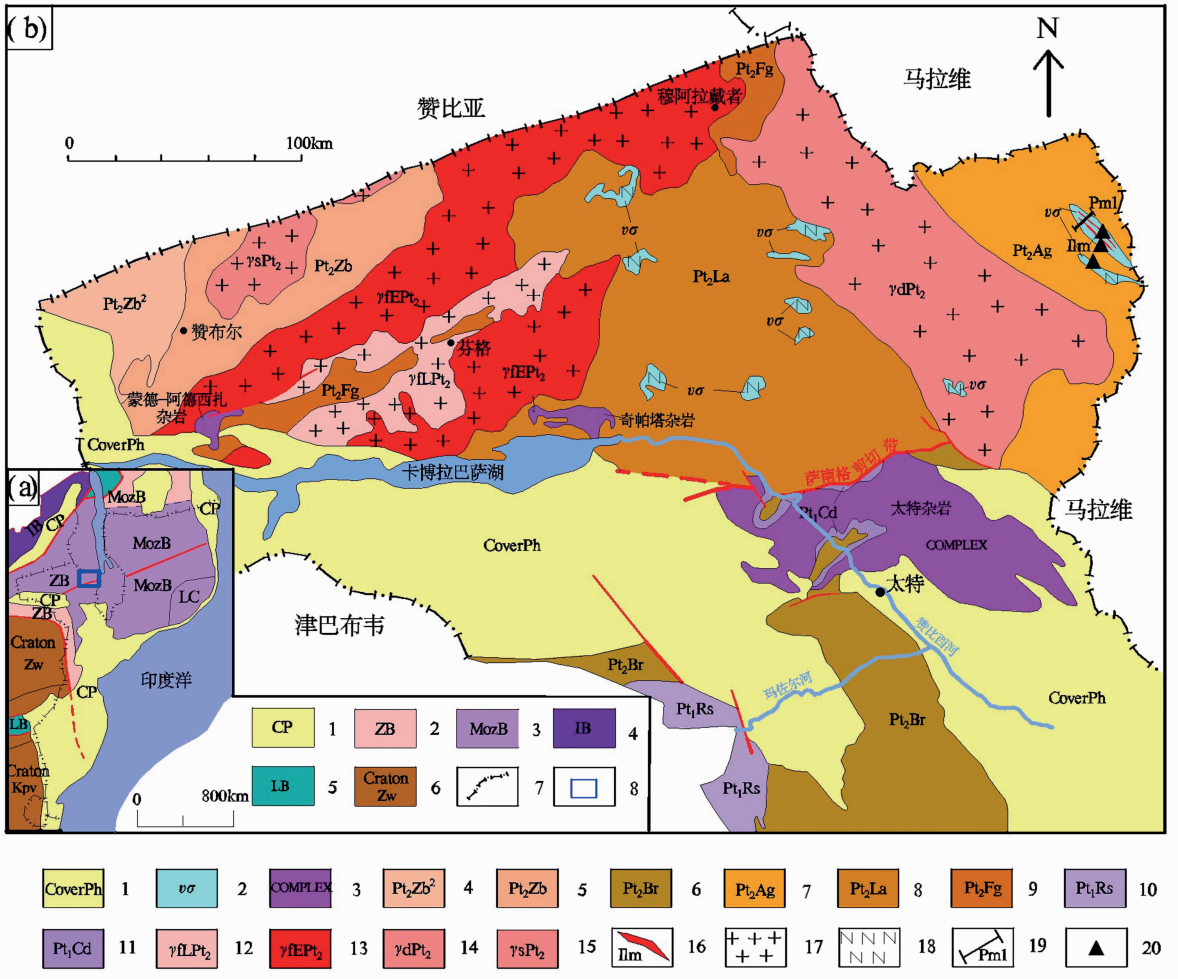


图 1 (a)—莫桑比克区域构造图;(b)—莫桑比克太特省地质略图((a)图据 Hanson,2003;(b)图据 Barr et al. ,1987,有修改)  
 Fig. 1 (a)—Regional structural map of Mozambique; (b)—geological map of Tete province in Mozambique (a modified after Hanson, 2003;b modified after Barr et al. ,1987)

(a)图:1—显生宙覆盖层;2—800~410Ma 泛非造山带;3—1.35-1.0Ga 造山带与 800~410Ma 泛非造山带;4—1.35~1.0Ga 造山带;5—2.05~1.8Ga 造山带;6—太古宙克拉通;7—国界;8—b 图位置;ZB—赞比西构造带;MozB—莫桑比克构造带;IB—依鲁米德造山带;LB—林波波造山带;LC—鲁依阿地块;(b)图:1—显生宙覆盖层;2—斜长岩;3—杂岩体;4—赞布尔岩群 2 组;5—赞布尔岩群;6—巴鲁岩群;7—安格尼亚岩群;8—鲁依阿岩群;9—芬格岩群;10—鲁辛喝岩群;11—希度尔岩群;12—晚芬格花岗岩;13—早芬格花岗岩;14—德萨朗哈马花岗岩;15—辛达花岗岩;16—钛铁矿体;17—花岗岩;18—斜长岩;19—剖面位置及编号;20—采样位置。

(a): 1—Phanerozoic overburden; 2—800~410Ma Pan-African orogenic belt; 3—1.35~1.0Ga orogenic and 800~410Ma Pan-African orogenic belt; 4—1.35~1.0Ga orogenic belt; 5—2.05~1.8Ga orogenic belt; 6—Archean craton; 7—national boundaries, 8—location for figure b; ZB—zambezi tectonic belt; MozB—Mozambican tectonic belt; IB—irumideorogenic belt; LB—Limpopo orogenic belt; LC—The Lluio block of LC; (b): 1—Phanerozoic overburden; 2—anorthosite; 3—composite pluton; 4—the Second Formation of Zambue Group; 5—Zambue Group; 6—Barue Group; 7—Angonia Group; 8—Luia Group; 9—Fingoe Group; 10—Rushinga Group; 11—Chidue Group; 12—Late Fingoe granite; 13—Early Fingoe granite; 14—Desaranhama granite; 15—Sinda granite; 16—Ilmenite ore body; 17—granite; 18—anorthosite; 19—section position and number; 20—sampling location

钛铁矿矿石光片 1 件。

钛铁矿光片镜下特征:它形晶结构、粒状结构;稠密浸染状,条带一块状构造。钛铁矿 60%,钛磁铁矿 20%,脉石矿物(斜长石)20%。岩石含大量金属矿物,光片中可见金属矿物主要为钛铁矿和钛磁铁矿。钛铁矿:他形晶,块状,灰色,较显著非均质性

(淡黄—暗蓝紫)。钛磁铁矿:他形晶粒状,暗灰色(相对钛铁矿),粒径约 0.3~2mm;常见交代钛铁矿,可见钛磁铁矿中包含细小残余的钛铁矿(图 3c)。

斜长岩薄片镜下特征:岩石为中粗粒镶嵌粒状结构,块状构造。斜长石 96%;角闪石 3%;钛铁矿 1%,斜长石它形粒状,粒径 1.5~3.8mm,有钠长石

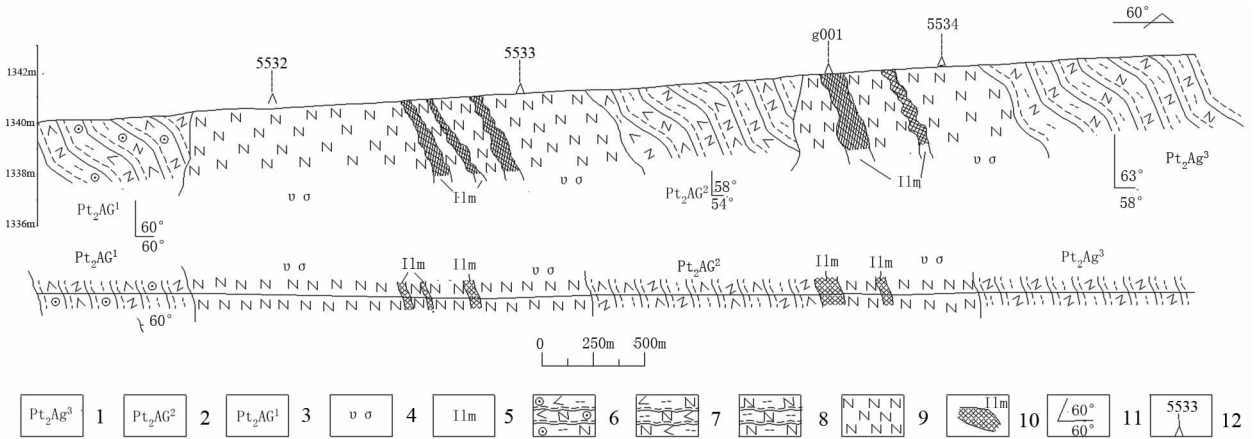


图 2 莫桑比克太特省钛铁矿田斜长岩实测剖面图(Pm1)

Fig. 2 Measured section for anorthosite in ilmenite field, Tete province, Mozambique (Pm1)

1—中元古代安格尼亚群 3 组;2—中元古代安格尼亚群 2 组;3—中元古代安格尼亚群 1 组;4—斜长岩体 5—钛铁矿体;

6—石榴黑云角闪斜长片麻岩;7—黑云角闪斜长片麻岩;8—黑云斜长片麻岩;9—斜长岩;10—钛铁矿;11—片麻理产状;12—采样位置

1—The Third Formation of the Mesoproterozoic Angonia Group; 2—the Second Formation of the Mesoproterozoic Angonia Group; 3—the First Formation of the Mesoproterozoic Angonia Group; 4—anorthosite intrusive body; 5—Ilmenite ore body; 6—garnet biotite amphibole gneiss; 7—biotite amphibole plagioclase gneiss; 8—biotite plagioclase gneiss; 9—anorthosite; 10—ilmenite; 11—gneiss occurrence; 12—sampling location

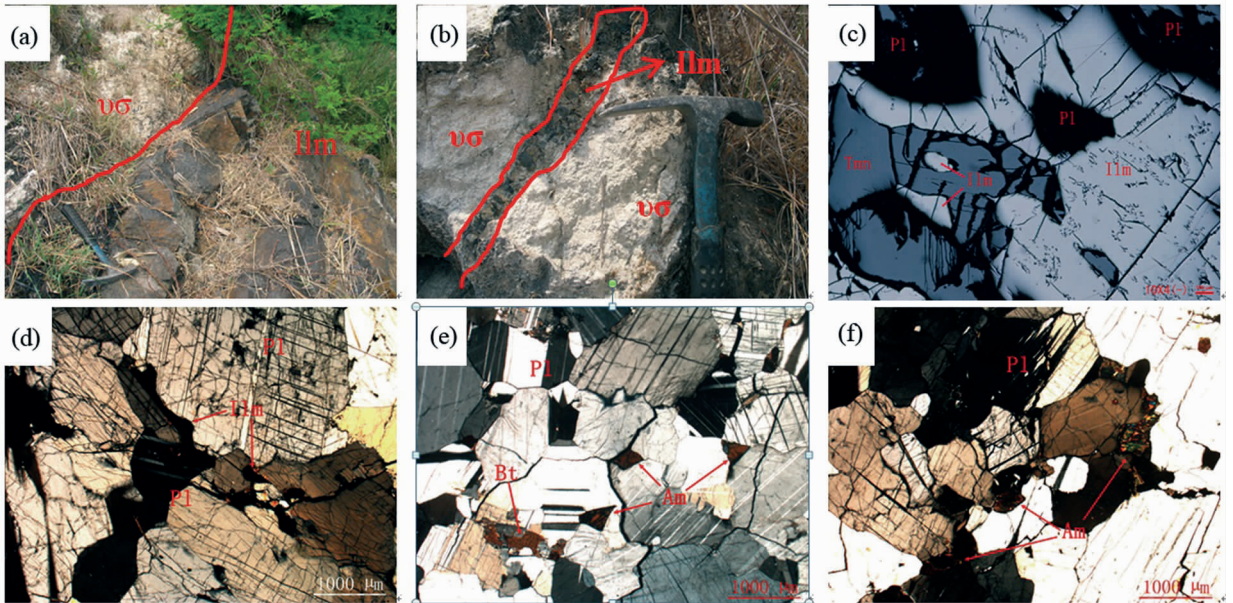


图 3 莫桑比克太特省钛铁矿田斜长岩野外及镜下特征(正交偏光)

Fig. 3 The pictures for field and microscopic of anorthosite in ilmenite field, Tete province, Mozambique (orthogonal polarized)

(a)—斜长岩与钛铁矿接触关系图;(b)—斜长岩中的钛铁矿夹层;(c)—钛铁矿显微照片;(d)—含钛铁矿斜长岩显微照片

(e)—含黑云母、角闪石斜长岩显微照片;(f)—含角闪石斜长岩显微照片

Ilm—钛铁矿;vσ—斜长岩;Tmn—钛磁铁矿;Pl—斜长石;Bt—黑云母;Am—角闪石

a)—Contact relationship between anorthosite and ilmenite; (b)—ilmenite intercalations in anorthosite; (c)—photomicrograph for ilmenite;

(d)—photomicrograph for anorthosite containing Ilmenite; (e)—photomicrograph for anorthosite containing biotite-and-amphibole;

(f)—photomicrograph for anorthosite containing hornblende

Ilm—Ilmenite; vσ—anorthosite. Tmn—titano-magnetite; Pl—anorthose; Bt—biotite; Am—amphibole

双晶及卡-钠复合双晶和肖钠长石-钠长石复合双晶。据 $\perp(010)$ 切面钠长石双晶最大对称消光角测定,为  $An = 38 \sim 50$  的中-拉长石。角闪石它形粒状,粒径  $0.1 \sim 0.5 \text{ mm}$ 。钛铁矿它形粒状,部分呈菱形,粒径  $0.1 \sim 0.3 \text{ mm}$ ,分散于岩石内(图 3d)。

部分斜长岩薄片,可见有角闪石、黑云母(图 3e、3f)等矿物。

### 3 采样位置及分析方法

本次在研究区内采集斜长岩薄片 5 件、化学全分析样、微量元素、稀土元素样各 5 件,

主要分布在剖面和钻探岩芯之中,样品采集均为无污染、风化程度较低的新鲜样品。于实测剖面中采得钛铁矿光片 1 件,并于钻孔中采得新鲜的斜长岩锆石 U-Pb 年龄样品 1 件(D103-1)。

#### 3.1 锆石 U-Pb 定年

锆石矿物的挑选、制靶、反射光和阴极发光照相是由中国冶金地质总局山东局测试中心实验室完成。斜长岩样品破碎后,经重液分选和电磁分离后在双目镜下挑选出锆石晶体,此后将锆石颗粒浇铸于环氧树脂靶中,磨蚀和抛光至锆石核部出露。再通过反射光和 CL 图像对挑好的锆石晶体形状和内部结构特征进行详细研究,之后选择无明显裂痕及包裹体的锆石测年。

锆石 U-Pb 同位素定年同样在中国冶金地质总局山东局测试中心实验室利用 LA-ICP-MS 分析完成。激光剥蚀过程中采用氦气作载气、氩气为补偿气以调节灵敏度,在等离子体中心气流中加入了少量氮气,以提高仪器灵敏度、降低检出限和改善分析精密度(Hu Zhaochu et al., 2008)。另外,对测试分析数据采用软件 ICP-MSDataCal(Liu Yongsheng et al., 2010)处理完成。U-Pb 同位素测年采用锆石标准 91500 进行同位素分馏校正,每分析 5 个样品点,至少分析 2~3 次 91500。锆石样品的 U-Pb 年龄谐和图和加权平均年龄计算均采用 Isoplot/Ex-ver3 (Ludwig, 2003)完成。

#### 3.2 岩石主微量元素

岩石主微量元素分析由南昌国土资源检测中心(江西省地质矿产勘查开发局实验测试中心)完成。主量元素( $\text{SiO}_2$ 、 $\text{TiO}_2$ 、 $\text{Al}_2\text{O}_3$ 、 $\text{Fe}_2\text{O}_3$ 、 $\text{FeO}$ 、 $\text{MnO}$ 、 $\text{MgO}$ 、 $\text{CaO}$ 、 $\text{Na}_2\text{O}$ 、 $\text{K}_2\text{O}$ 、 $\text{P}_2\text{O}_5$ )采用 X 荧光光谱法 [AFS-2100 型(D460)、PW2403 型(D183)]分析,精度优于 2%,检测下限为 0.01%。稀土元素、微量元素采用电感耦合等离子体质谱仪(ICP-MS X2 型)

进行测定,测定精密度优于 5%,检测下限为  $0.05 \mu\text{g/g}$ 。分析结果及特征参数见表 1、表 2。

表 1 莫桑比克太特省钛铁矿田斜长岩岩石主量元素化学成分表

Table 1 Contents of major element for anorthosites in ilmenite field, Tete province, Mozambique

采样号	5332	5333	5334	5397	
名称	斜长岩	斜长岩	斜长岩	斜长岩	
主量元素含量 (%)	$\text{SiO}_2$	49.42	50.94	50.49	52.56
	$\text{Al}_2\text{O}_3$	26.05	29.28	28.15	19.96
	$\text{TiO}_2$	1.09	0.21	0.46	0.7
	$\text{Fe}_2\text{O}_3$	1.09	0.089	0.16	0.66
	$\text{FeO}$	4.79	1.34	2.45	5.23
	$\text{K}_2\text{O}$	0.44	0.31	0.38	0.56
	$\text{Na}_2\text{O}$	3.65	3.54	3.42	3.65
	$\text{MgO}$	1.45	1.01	1.52	5.42
	$\text{CaO}$	10.35	12.51	12.23	10.22
	$\text{P}_2\text{O}_5$	0.3	0.044	0.063	0.062
	$\text{MnO}$	0.13	0.042	0.055	0.13
	LOI	1.2	0.63	0.59	0.81
	Total	99.96	99.95	99.97	99.96
$\text{Mg}^\#$	15.37	31.14	27.13	38.34	
$\text{FeO}_7/\text{MgO}$	3.65	1.27	1.55	0.98	
$\text{Na}_2\text{O} / \text{K}_2\text{O}$	8.30	11.42	9.00	6.52	

## 4 分析测试结果

#### 4.1 锆石 U-Pb 定年

斜长岩中的锆石多为无色透明长柱状或浑圆状,粒度多在  $50 \sim 100 \mu\text{m}$  之间,长宽比  $1:1 \sim 1:3$ , CL 图像(图 4)显示大部分锆石内部板状或杉树叶状分带,为典型基性岩浆成因锆石;少部分锆石边部非常窄,发光幔部稍亮,可能为更晚期生长的锆石。

锆石核幔部的 Th、U 和 Pb 含量范围分别为  $22 \times 10^{-6} \sim 176 \times 10^{-6}$ 、 $90 \times 10^{-6} \sim 341 \times 10^{-6}$  和  $9 \times 10^{-6} \sim 37 \times 10^{-6}$ (见表 3)。Th/U 比值介于  $0.24 \sim 0.52$  之间,指示其为岩浆成因(Wu Yuanbao et al., 2004)。如图 4 所示,斜长岩中锆石数据均落在谐和线上或附近(谐和度大于 92%)(图 5),核部  $^{206}\text{Pb}/^{238}\text{U}$  年龄介于  $561 \sim 599 \text{ Ma}$  之间,25 个数据点加权平均年龄为  $580 \pm 5 \text{ Ma}$ ,  $\text{MSWD} = 1.5$ ,代表了斜长岩的结晶年龄。

#### 4.2 岩石化学特征

斜长岩中  $\text{SiO}_2 = 49.42\% \sim 52.56\%$ ,为基性岩范围; $\text{Al}_2\text{O}_3 = 19.96\% \sim 29.28\%$ ,具有高铝的特征; $\text{TiO}_2$  含量为  $0.089\% \sim 1.09\%$ , $\text{K}_2\text{O}$  含量  $0.31\% \sim 0.56\%$ , $\text{MgO}$  含量  $1.01\% \sim 5.42\%$ , $\text{Mg}^\#$  指数为  $15.37 \sim 38.34$ ,显示具有低 Ti、K、Mg、Fe 特征; $\text{CaO}$  含量  $10.22\% \sim 12.51\%$ ,相对较高; $\text{Na}_2\text{O}$  含量

3.42%~3.65%,  $\text{Na}_2\text{O}/\text{K}_2\text{O}$  值为 6.52~11.42,  $\text{FeO}_7/\text{MgO}$  值为 0.98~3.65, 显示具有基性拉斑玄武岩特征。岩石 LOI 含量为 0.59%~1.2%, 挥发组分平均小于 1%(表 1)。

表 2 莫桑比克太特省钦铁矿田斜长岩稀土、微量元素地球化学成分及特征表

Table 2 Geochemical components and characteristics of rare earth and trace elements for anorthosites in ilmenite field, Tete province, Mozambique

采样号	5332	5333	5334	5397	
名称	斜长岩	斜长岩	斜长岩	斜长岩	
稀土元素含量 ( $\times 10^{-6}$ )	Y	6.97	2.13	4.28	9.98
	La	4.82	3.07	3.63	6.61
	Ce	9.5	5.98	7.35	14.9
	Pr	1.27	0.72	0.97	2
	Nd	5.14	2.91	4.16	8.6
	Sm	1.12	0.61	1.04	2.13
	Eu	1.5	0.98	1.13	1.32
	Gd	1.18	0.43	0.84	1.91
	Tb	0.21	0.077	0.15	0.35
	Dy	1.37	0.5	0.84	1.93
	Ho	0.24	0.075	0.16	0.39
	Er	0.75	0.24	0.51	1.2
	Tm	0.12	0.041	0.067	0.17
	Yb	0.72	0.26	0.5	1.28
	Lu	0.12	0.041	0.085	0.22
	$\text{La}_N/\text{Yb}_N$	3.98	5.84	3.69	2
$\text{Ce}_N/\text{Yb}_N$	3.47	6.06	3.87	3.06	
$\delta\text{Eu}$	4.56	8.04	4.94	3.51	
$\Sigma\text{REE}$	28.06	15.93	21.43	43.01	
LREE/HREE	11.91	8.27	21.44	12.42	
微量元素含量 ( $\times 10^{-6}$ )	Nb	7.85	4.81	5.43	6.96
	Ta	0.36	0.12	0.21	0.17
	Rb	1.65	3.8	3	4.1
	Sr	469	453	457	398
	Ni	4.52	6.97	7.51	11.5
	Co	10.7	6.2	9.47	24
	U	0.12	0.11	0.13	0.2
	Ba	184	132	127	188
	Zr	32.5	26.6	31	46.5
	As	0.53	0.44	0.32	0.2
	Th	1.13	0.58	1.17	2.31
	Hf	1.39	0.79	0.98	1.75
	Sc	7.94	2.18	5.14	24.6
	Sb	0.097	0.12	0.1	0.067
	Th/Hf	0.81	0.73	1.19	1.32
	Ta/Hf	0.26	0.15	0.21	0.10
Th/Ta	3.14	4.83	5.57	13.59	
Zr/Y	4.66	12.49	7.24	4.66	

在  $(\text{Na}_2\text{O} + \text{K}_2\text{O}) - \text{SiO}_2$  图解(图 6a)中, 岩石落入玄武岩、玄武质安山岩类岩石范围内; 在  $\text{K}_2\text{O} - \text{SiO}_2$  图解(图 6b)中, 岩石落入低钾拉斑玄武岩范围内。

## 4.3 地球化学特征

### 4.3.1 稀土元素特征

斜长岩中稀土元素总量为  $15.93 \times 10^{-6} \sim 43.01 \times 10^{-6}$ (表 2), 显示稀土总量相对较低,  $\text{La}_N/\text{Yb}_N$  值为 2~5.84, 轻、重稀土分馏一般,  $\text{Ce}_N/\text{Yb}_N$  值为 3.06~6.06, 具有岩石圈地幔的高度部分熔融分异特征; 轻重稀土比值为 8.27~21.44, 轻稀土具有一定的富集;  $\delta\text{Eu}$  变化于 3.51~8.04, 具有明显的 Eu 元素富集, 体现了斜长石矿物的特性。

在稀土配分曲线图中(图 7a), 斜长岩样品的曲线分布形态相似, 均向右倾, 显示轻稀土较为富集, 重稀土元素较平缓, 轻、重稀土分馏不是特别明显; Eu 主要表现为正异常-高正异常, 显示岩浆较高的分异程度。

### 4.3.2 微量元素特征

斜长岩样品微量元素含量总体高于原始地幔值(表 2), 仅有个别不相容元素(Y、Yb、Lu)含量相当或低于原始地幔值。Th/Hf 比值为 0.81~1.32, 平均为 1.1, Ta/Hf 比值为 0.1~0.26, 平均为 0.18, Th/Ta 比值为 3.14~13.59, 平均值为 7 左右, Zr/Y 比值为 4.66~12.49, 各微量元素含量及特征值见表 2。

原始地幔标准化蛛网图(图 7b)显示, 斜长岩样品微量元素分配曲线一致, 代表同源岩浆结晶分异特征。岩石样品具有明显的大离子亲石元素 Ba、Sr 元素的富集, Pb 元素的富集, 高场强元素 Zr、Nb 等元素的亏损, 显示为大陆玄武岩特征。

## 5 讨论

### 5.1 斜长岩成因分析

研究区内的斜长岩中主要矿物以中-拉长石为主( $\text{An}_{38} \sim \text{An}_{50}$ ), 具有低 K、Mg、Fe, 高 Ca、Al 岩石化学特征, 虽部分元素含量受斜长岩矿物组分影响明显, 但总体能够反映低钾拉斑玄武质特征。区内斜长岩成因环境与河北大庙的斜长岩相似, 可能均为拉斑玄武质岩浆的结晶分异(Hu Shiling et al., 1990), 同时岩浆的侵位过程也并非单一过程, 应当具有同期多阶段的侵位特征(Chen Zhengle et al., 2014)。玄武质岩浆一般来源于岩石圈地幔或软流圈(Sklyarov et al., 2003; Kong Huilei et al., 2018), 其中岩石圈地幔相对富集 LILE 和 LREE, 亏损高场强元素 Nb、Ta、Zr; 软流圈地幔则相对富集大离子亲石元素和高场强元素。斜长岩样品的数据具有 LREE 富集和 Rb、Sr、Ba 等大离子亲石元素

表3 莫桑比克太特省钛铁矿田斜长岩锆石 U-Pb 测年结果表

Table 3 Zircons U-Pb dating results for anorthosites in ilmenite field, Tete province, Mozambique

测点	位置	元素含量( $\times 10^{-6}$ )和比值				同位素比值					年龄(Ma)				谐和度
		Pb	Th	U	Th/U	$^{207}\text{Pb}/^{235}\text{U}$	$\pm 1\delta$	$^{206}\text{Pb}/^{238}\text{U}$	$\pm 1\delta$	rho	$^{207}\text{Pb}/^{235}\text{U}$	$\pm 1\delta$	$^{206}\text{Pb}/^{238}\text{U}$	$\pm 1\delta$	
1	核部	19	51	176	0.29	0.775	0.030	0.0947	0.0017	0.46	583	17	583	10	99%
2	幔部	12	31	112	0.27	0.731	0.034	0.0908	0.0018	0.43	557	20	560	11	99%
3	幔部	10	22	91	0.24	0.710	0.039	0.0934	0.0022	0.42	545	23	575	13	94%
4	幔部	17	43	159	0.27	0.747	0.030	0.0956	0.0019	0.49	567	18	588	11	96%
5	幔部	20	58	187	0.31	0.740	0.030	0.0949	0.0015	0.40	562	18	584	9	96%
6	幔部	18	47	169	0.28	0.812	0.033	0.0956	0.0020	0.51	604	18	588	12	97%
7	核部	16	40	156	0.26	0.753	0.032	0.0914	0.0016	0.40	570	19	564	9	98%
8	幔部	16	45	151	0.30	0.784	0.032	0.0951	0.0019	0.49	588	18	586	11	99%
9	幔部	16	36	149	0.24	0.791	0.033	0.0940	0.0018	0.46	592	19	579	11	97%
10	核部	20	55	183	0.30	0.791	0.032	0.0952	0.0015	0.40	592	18	586	9	99%
11	幔部	21	58	191	0.30	0.784	0.030	0.0974	0.0021	0.56	588	17	599	12	98%
12	核部	22	65	200	0.33	0.766	0.028	0.0967	0.0017	0.47	578	16	594	10	97%
13	幔部	13	32	127	0.25	0.722	0.030	0.0910	0.0016	0.42	552	18	561	10	98%
14	幔部	19	46	168	0.27	0.833	0.030	0.0973	0.0016	0.44	615	17	599	9	97%
15	核部	23	80	207	0.39	0.740	0.027	0.0933	0.0016	0.45	563	16	575	9	97%
16	幔部	13	32	123	0.26	0.808	0.032	0.0948	0.0017	0.44	601	18	584	10	97%
17	核部	38	176	341	0.52	0.754	0.025	0.0912	0.0014	0.47	570	15	563	8	98%
18	核部	25	82	232	0.35	0.715	0.024	0.0917	0.0016	0.51	548	14	566	9	96%
19	核部	24	76	217	0.35	0.879	0.028	0.0967	0.0015	0.49	640	15	595	9	92%
20	核部	22	58	206	0.28	0.786	0.026	0.0939	0.0014	0.47	589	15	579	9	98%
21	幔部	14	33	125	0.26	0.802	0.040	0.0957	0.0017	0.35	598	23	589	10	98%
22	幔部	18	46	169	0.27	0.793	0.028	0.0935	0.0015	0.44	593	16	576	9	97%
23	幔部	13	33	126	0.26	0.795	0.033	0.0927	0.0016	0.42	594	19	572	10	96%
24	幔部	13	40	122	0.33	0.814	0.030	0.0962	0.0017	0.49	605	17	592	10	97%
25	幔部	13	30	125	0.24	0.790	0.032	0.0935	0.0016	0.41	591	18	576	9	97%

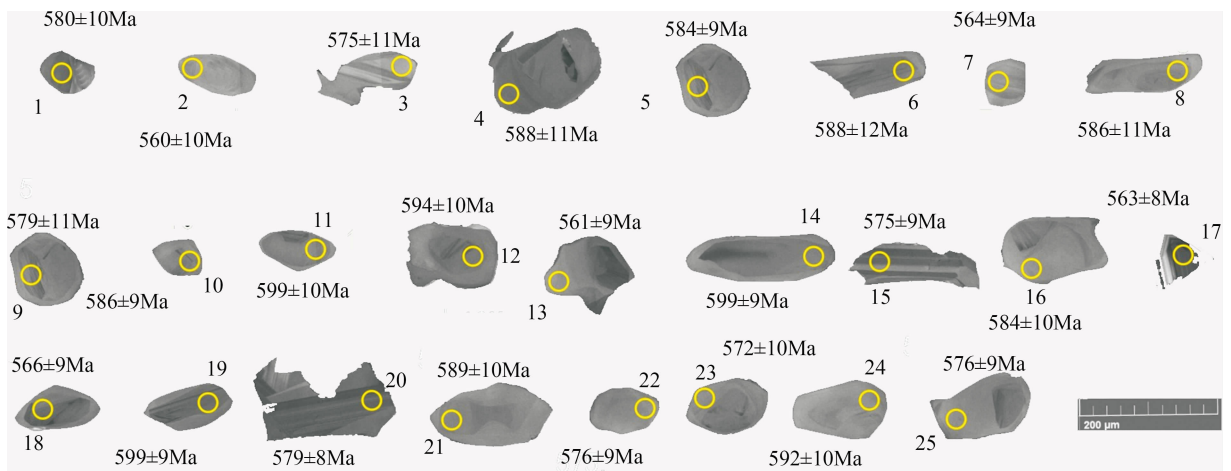


图4 莫桑比克太特省钛铁矿田斜长岩锆石阴极发光照片(D103-1)

Fig. 4 Cathodoluminescence (CL) images for zircons from anorthosite in ilmenite field, Tete province, Mozambique (D103-1)

的富集, Nb、Ta、Zr 等元素的亏损, 反映了岩石具有岩石圈地幔的特征。

泛非造山运动之前, 南部非洲大陆的地壳厚度相对较薄 (< 20 ~ 30 km) (Ziegler et al., 2004; Jean Chorowicz, 2005), 初步判断认为研究区内斜长岩的形成可能存在两种模式: ① 不含钛铁矿斜长岩。为

上地幔或下地壳, 在板块俯冲脱水而致使熔点降低 (亏损 Nb、Ta) 作用的影响, 而高度熔融分离后形成拉斑玄武岩质岩浆, 在岩浆热液上移过程中, 由于温度和压力以及氧逸度不一致, 导致辉石以及角闪石的结晶, 残余岩浆则为富集斜长石熔体, 之后漂浮岩浆顶部, 通过压滤作用将内部熔体挤出, 形成斜长岩

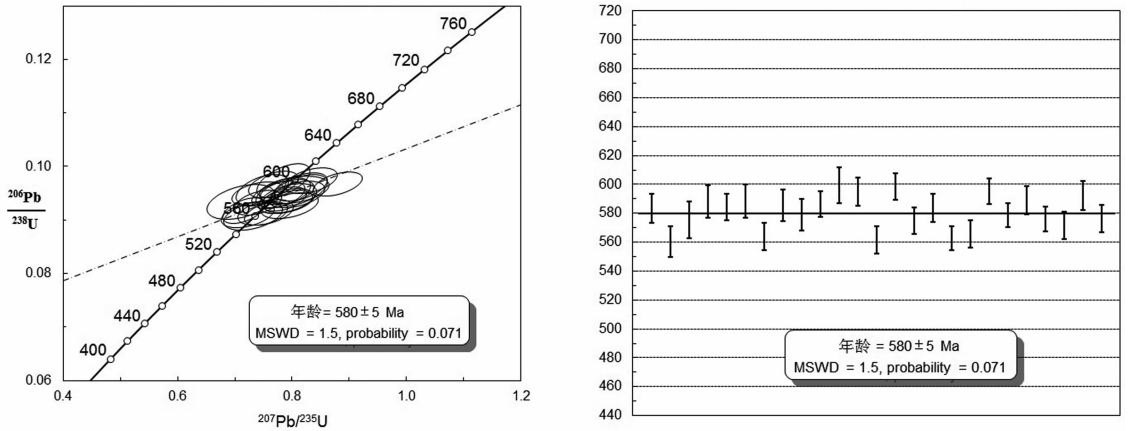


图 5 莫桑比克太特省钛铁矿田斜长岩锆石 U-Pb 同位素年龄谱和图(D103-1)

Fig. 5 Zircon U-Pb concordia diagrams from anorthosite in ilmenite field, Tete province, Mozambique (D103-1)

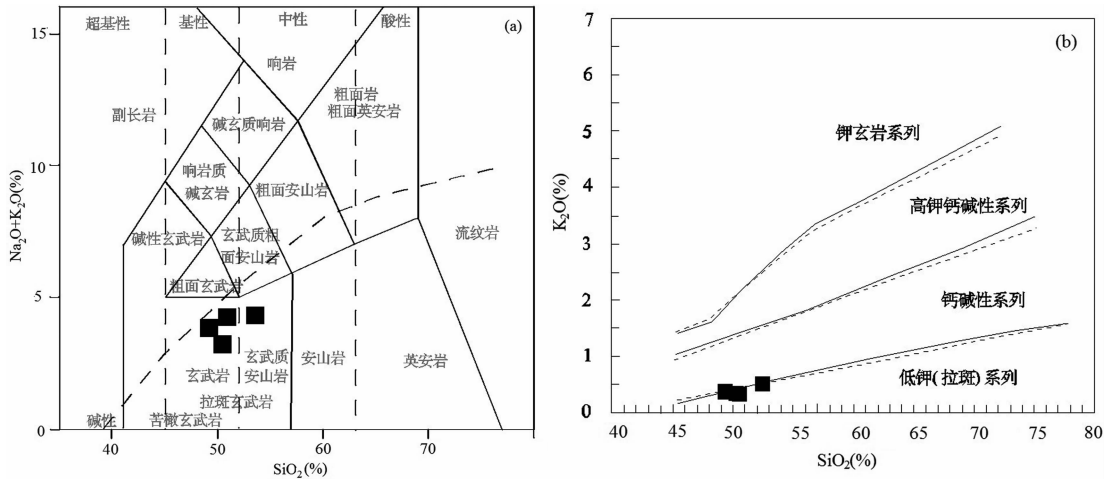


图 6 莫桑比克太特省钛铁矿田斜长岩 (Na<sub>2</sub>O+K<sub>2</sub>O)-SiO<sub>2</sub> (a) 和 K<sub>2</sub>O-SiO<sub>2</sub> (b) 图解

(a. 据 Le Bas et al., 1986; b. 实线据 Pecerrillo et al., 1976, 虚线据 Middlemost, 1985)

Fig. 6 (Na<sub>2</sub>O+K<sub>2</sub>O)-SiO<sub>2</sub> (a) and K<sub>2</sub>O-SiO<sub>2</sub> (b) diagram for anorthosite in ilmenite field, Tete province, Mozambique

(a. after Le Bas et al., 1986; b. Solid line after Pecerrillo et al., 1976, dash line after Middlemost, 1985)

体;②富集钛铁矿斜长岩岩浆。总体形成模式和前者类似,其热量来源也有可能为俯冲脱水作用或者为地幔热柱,漂浮岩浆顶部的含矿斜长岩岩浆,通过压滤作用将钛铁矿岩浆挤压到应力最小位置,从而结晶分异形成钛铁矿和斜长岩(Emslie et al., 1994; Lindsley et al., 2010)。

### 5.2 钛铁矿成因、成矿模式与时代分析

河北大庙钛铁矿形成于 1.74Ga,为典型的斜长岩钛铁矿床(Hu Shiling et al., 1990; Chen Zhengle et al., 2014; Chen Terry Wei et al., 2016),其矿床成因模式为岩浆晚期分离结晶贯入式、分凝结晶式,但也有学者认为岩浆晚期结晶分异压滤模式与蚀变再活化的迁移模式(Zhang Zhaochong, 2018; Li Xingli et al., 2019)。山东莒县钛铁矿则为新太

古代之后,岩浆晚期分异型钛铁矿(Zhang Lianfeng et al., 2006),其含矿岩层主要为钛铁矿角闪石岩。挪威南部罗加兰(Rogaland)钛铁矿形成于 931.5Ma,920.3Ma(Charlier et al., 2006),为新元古代,也为典型的斜长岩型钛铁矿床,有学者认为该矿床成因为岩浆分步结晶分异型(Schaerer et al., 1996; Duchesne, 1999),也有学者认为其为岩浆晚期结晶分异压滤模式(Charlier et al., 2015)。加拿大拉布拉多(Labrador)斜长岩型的钛铁矿床,斜长岩形成时代为 1625Ma(Kerr et al., 2013),其成因类型为晚期结晶分异型,并分为三个相变过程。

前人对莫桑比克太特省钛铁矿及斜长岩做了少量的研究,有学者认为莫桑比克斜长岩型钛铁矿形成时代主要为 1730Ma 与 600~800Ma 两个时期

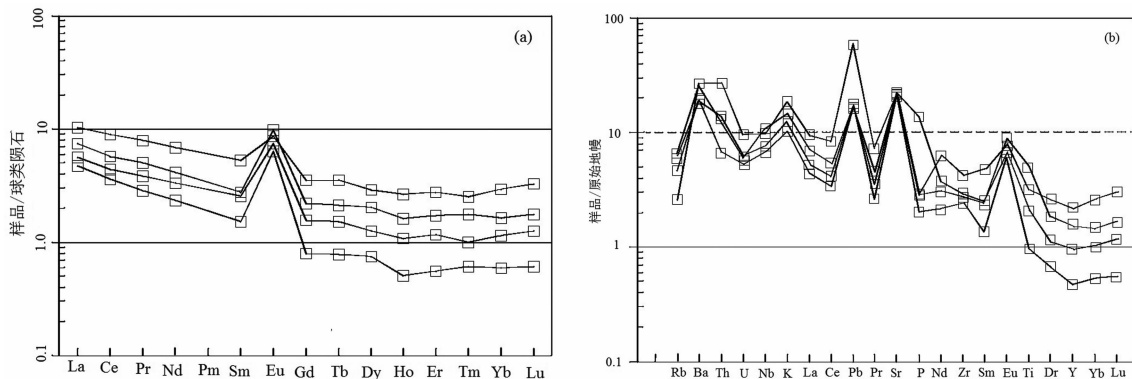


图7 莫桑比克太特省钛铁矿田斜长岩稀土元素球粒陨石标准化配分曲线图(a)

及微量元素原始地幔标准化蛛网图(b)(标准化数值据 Sun et al., 1989)

Fig. 7 Chondrite-normalized REE patterns(a) and primitive mantle-normalized trace element patterns (b) for anorthosite in ilmenite field, Tete province, Mozambique(normalizing values after Sun et al., 1989)

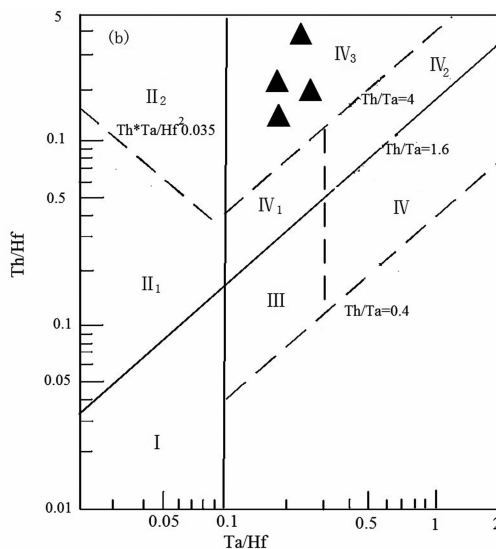
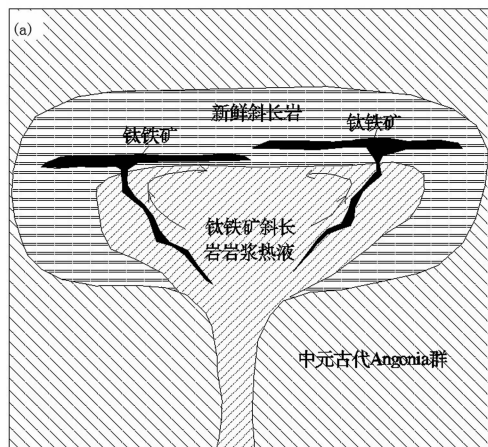


图8 莫桑比克太特省斜长岩钛铁矿形成的压滤模式图(a)及斜长岩 Th/Hf-Ta/Hf 构造环境判别图(b)

(a 图据 Charlier et al., 2015, 有修改; b 图据 Wang Yunliang et al., 2001, 有修改)

Fig. 8 Pressure filtration mineralization model of anorthosite-ilmenite (a) and Th/Hf-Ta/Hf tectonic environment discrimination diagram for anorthosite (b) in Tete province, Mozambique

(a—modified after Charlier et al., 2015; b—modified after Wang Yunliang et al., 2001)

b: I—板块发散边缘, N-MORB 区; II—板块汇聚边缘; (III—大洋岛弧玄武岩区; II2—陆缘岛弧及陆缘火山弧玄武岩区); III—大洋板内洋岛、海山玄武岩区及 T-MORB、E-MORB 区; IV—大陆板内 (IV1—陆内裂谷及陆缘裂谷拉斑玄武岩区; IV2—陆内裂谷碱性玄武岩区; IV3—大陆拉张带(或初始裂谷)玄武岩区); V—地幔热柱玄武岩区

b: I—Divergent edge of the plate, N-MORB region; II—plate convergence edge (III—Oceanic island arc basalt zone; II2—epicontinental island arc and epicontinental volcanic arc basalt zone); III—intraoceanic island, Seishan basalt zone, T-MORB and E-MORB zone; IV—continental plate (IV1—intracontinental rift and marginal rift Tholeiite zone; IV2—intracontinental rift alkaline basalt zone; IV3—continental extensional belt (or initial rift) basalt zone); V—mantle plume basalt region

(Andreoli, 1984); 但又有学者通过测定钛铁矿共生斜长岩 Rb-Sr、Sm-Nd 同位素年龄, 认为其形成时代为 1144Ma 及  $588 \pm 26\text{Ma}$  (Barr et al., 1984; Evans et al., 1999)。有学者初步认为研究区内钛铁矿为新元古代岩浆早期结晶分异型 (He Heling et al.,

2012); 也有学者初步认为是岩浆结晶分异与重力分异型 (Xiao Xiaolin et al., 2014), 并划分为早期重力分异式与晚期贯入式两个成矿阶段。

本文获得与钛铁矿共生斜长岩锆石 U-Pb 年龄为  $580 \pm 5\text{Ma}$ , 反映了钛铁矿成矿的精确时代, 其与

区内、莫桑比克构造带内莫马(Moma)一带以及邻国马达加斯加(Madagascar)大量的 600~550Ma 斜长岩钦铁矿(Ashwal et al., 1998; Jacobs et al., 1998)具有较好的一致性。作者认为,研究区内斜长岩型钦铁矿为岩浆晚期结晶分异型,其成矿模式为:结晶分异压滤模式(图 8a),其成矿机制与斜长岩成因模式一致。即成矿母岩浆在深部聚集形成含矿岩浆热液并发生分异作用,随后密度较低的中—拉长石( $An_{38} \sim An_{50}$ )漂浮在岩浆房的顶部,钦铁氧化物、斜长石热液岩浆一起随后底辟式上升,最后通过压滤作用将铁钦氧化物挤压到斜长岩应力最弱处,最后分离结晶而成。

### 5.3 斜长岩构造环境分析

稀土元素和微量元素是相对较为稳定的元素,特别是 Zr、Hf、Nb、Ta、Th 等高场强元素能够较好地示踪岩石的成因及构造环境(Hanson, 1980; Ganzeyev et al., 1984; Sun Jiming et al., 2018; Kong Huilei et al., 2018)。研究区内斜长岩中具有 Pb 元素富集, Nb、Ta 元素亏损为典型大陆玄武岩的特征; Zr/Y 比值为 4.66~12.49(大于 4),也显示比值远大于岛弧火山岩而类似于板内玄武岩(Sun Jiming et al., 2018);另外斜长岩中的大离子亲石元素 K、Rb、Sr、Cs 的富集,高场强元素 Zr、Hf、Nb、Ta 等的亏损,尤其为 Nb、Ta 亏损暗示着岩浆的来源受俯冲岩石圈的影响(Davis et al., 1995),同时低 Ti 特征暗示其形成与大陆内岩石圈伸展有关,且受到消减带物质的影响(West et al., 2004; Orozco-Esquivel et al., 2007; Gazel et al., 2012)。区内斜长岩中 Ta/Hf 比值为 0.1~0.21(大于 0.1, 小于 0.3),显示为拉斑玄武岩特征(Shinjo et al., 1999; Wang Yunliang et al., 1984); Th/Ta 平均比值为 7 (>1.6),判定其为陆内拉张或初始裂谷玄武岩特征(图 8b)。综上所述,研究区内的斜长岩为弧后伸展构造环境(图 9)。

## 6 结论

(1)研究区斜长岩具有亏损 Ti、Zr、Nb 元素,富集大离子亲石元素、Pb 元素, Ta/Hf 比值为 0.1~0.21 等特征,显示了典型贫 Ti 大陆拉斑玄武岩的特征;通过岩石地球化学特征,综合判定其形成构造环境为陆内弧后伸展构造环境。

(2)经 LA-ICP-MS 测得其锆石 U-Pb 年龄为  $580 \pm 5$  Ma, 显示了斜长岩形成的时代为新元古代晚期,同时也揭露了钦铁矿的大致成矿时代。

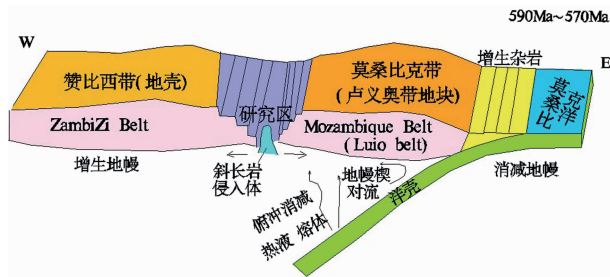


图 9 莫桑比克太特省钦铁矿田 590~570Ma 构造环境反演示意图

Fig. 9 The diagram for Inversion schematic tectonic environment from 590Ma to 570Ma in ilmenite field, Tete province, Mozambique

(3)在系统的总结和对比全球斜长岩型钦铁矿矿床的基础上,结合区内研究资料认为,研究区内钦铁矿成矿事件 1~2 次。斜长岩型钦铁矿的矿床成因为岩浆晚期结晶分异型,其成矿模式为晚期结晶分异压滤模式。

(4)研究区同时叠加了中元古代造山事件和新元古代—早古生代泛非造山事件,赞比西构造带从中元古代到早古生代为连续的造山阶段;同时本次研究作为莫桑比克赞比西构造带 660~610Ma 泛非造山运动提供了重要证据。

**致谢:**感谢匿名评审专家以及责任编辑对本文提出了非常宝贵的修改意见;同时感谢中国地质调查局天津地调中心任军平高级工程师,南京大学地球科学与工程学院朱文斌教授、郑碧海博士、朱米西硕士,中国地质科学院田作林博士后对本文的指导与支持。

## References

- Ashwal L D, Hamilton M A, Morel V P I, Rambeloson R A. 1998. Geology, petrology and isotope geochemistry of massif-type anorthosites from southwest Madagascar. *Contributions to Mineralogy and Petrology*, 133:389~401.
- Ashwal L D, Armstrong R A, Roberts R J, Schmitz M D, Corfu F, Hetherington C J, Burke K, Gerber M. 2007. Geochronology of zircon megacrysts from nepheline bearing gneisses as constraints on tectonic setting: implications for resetting of the U-Pb and Lu-Hf isotopic systems. *Contributions to Mineralogy and Petrology*, 153:389~403.
- Andreoli M A G. 1984. Petrochemistry, tectonic evolution and metasomatic mineralisations of Mozambique belt granulites from S. Malawi and Tete (Mozambique). *Precambrian Research*, 25:161~186.
- Anne Grunow, Richard Hanson, Terry Wilson. 1996. Were aspects of Pan-African deformation linked to Iapetus opening?. *Geological Society of America*, 24:1063~1066.
- Barr M W C, Downing K N, Harding A E, Loughlin W P. 1984. Regional correlation near the junction of the Zambezi and Mozambique Belts, east-central Africa. *Hunting Geology and Geophysics*, 77~78.

- Barr M W C, Brown M A. 1987. Precambrian gabbroanorthosite complexes, Tete Province, Mozambique. *Geological Journal*, 22:139~159.
- Beaumont C, Jamieson R A, Butler J P, Warren C J. 2009. Crustal structure: a key constraint on the mechanism of ultra-high-pressure rock exhumation. *Earth and Planetary Science Letters*, 287:116~129.
- Bjerkgård T, Stein H J, Bingen B, Henderson I H C, Sandstad J S, Moniz A. 2009. The Niassa Gold Belt, northern Mozambique—a segment of a continental-scale Pan-African gold-bearing structure? *Journal of African Earth Sciences*, 53:45~58.
- Bingen B, Jacobs J, Viola G, Henderson I H C, Skårø, Boyd R, Thomas R J, Solli A, Key R M, Daudi. 2009. Geochronology of the Precambrian crust in the Mozambique belt in NE Mozambique, and implications for Gondwana assembly. *Precambrian Research*, 170(3):231~255.
- Brito Neves B B, Campos Neto M C, Fuck R A. 1999. From Rodinia to Western Gondwana: an approach to the Brasiliano-Pan African cycle and orogenic collage. *Episodes*, 22: 155~166.
- Charlier B, Duchesne J C, Vander Auwera J. 2006. Magmochamber processes in the Tellnesilmenite deposit (Rogaland Anorthosite Province, SW Norway) and the formation of Fe-Ti ores in massif-type anorthosites. *Chemical Geology*, 234:264~290.
- Charlier B, Namur O, Bolle O, Latypov R, Duchesne J C. 2015. Fe-Ti-V-P ore deposits associated with Proterozoic massif-type anorthosites and related rocks. *Earth-Science Reviews*, 141:56~81.
- Chen Terry Wei, Zhao Taiping. 2016. Origin of the ~1.74 Ga, Anorthosite-hosted Damiao Fe-Ti-P Ore Deposit, North China. *Acta Geologica Sinica (English Edition)*, 90(S1):188.
- Chen Zhengle, Chen Bailin, Li Houmin, Du Weihe, Li Lixing, Hang Fengbin, Wang Yong, Sun Yue, Wu Yue, Zhang Wengao. 2014. Geological Characteristics of the Damiao Iron Deposit, North China Craton and Ore-Prospecting. *Acta Geologica Sinica*, 88(12):2339~2350 (in Chinese with English abstract).
- Costa M, Ferrara G, Sacchi R, Tonarini I S. 1992. Rb/Sr dating of the Upper Proterozoic basement of Zambesia, Mozambique. *Geologische Rundschau*, 81:487~500.
- Collins A S, Pisarevsky S A. 2005. Amalgamating eastern Gondwana: the evolution of the Circum-Indian Orogens. *Earth Science Reviews*, 71:229~270.
- Cutten H N C, Johnson S P. 2006. Tectonic evolution of the Mozambique Belt, eastern Africa. *Maputo Conference, abstracts*, 33~34.
- Dalziel I W D. 1994. Precambrian Scotland as a Laurentia-Gondwana link; Origin and significance of cratonic promontories. *Geology*, 22:587~590.
- Davis J M, Hawkesworth C J. 1995. Geochemical and tectonic transitions in the evolution of the Mogollon-Datil Volcanic Field, New Mexico, U S A. *Chemical Geology*, 119(1-4):31~53.
- De Wit M J, Bowring S A, Ashwal L D, Randrianasolo L G, Morel V P I, Rambeloson R A. 2001. Age and tectonic evolution of Neoproterozoic ductile shear zones in southwestern Madagascar, with implications for Gondwana studies. *Tectonics*, 20:1~45.
- Deng Yutao, Yang Ruiru, Zhang Zhao, Han Zhihua, Li Li. 2017. Geological characteristics of binhai Heavy placer in Mozambique. *China Coal Geology*, 29(12): 31~35. (in Chinese with English abstract).
- Diot H, Bolle O, Lambert J M, Launeau P, Duchesne J C. 2003. The Tellnesilmenite deposit (Rogaland, South Norway): Magnetic and petrofabric evidence for emplacement of a Ti-enriched noritic crystal mush in a fracture zone. *Journal of Structural Geology*, 25:481~501.
- Druppel K, Seckendorff V, Okrusch M. 2001. Subsolidus reaction textures in the anorthositic rocks of the southern part of the Kunene intrusive complex, NW Namibia. *European Journal of Mineralogy*, 13:238~309.
- Duchesne J C. 1999. Fe-Ti deposits in Rogaland anorthosites (South Norway): geochemical characteristics and problems of interpretation. *Mineralium Deposita*, 34:182~198.
- Emslie R F, Hamilton M A, Thériault R J. 1994. Petrogenesis of a Mid Proterozoic Anorthosite-mangerite-charnockite-granite (AMCG) complex: Isotopic and chemical evidence from the Nain Plutonic Suite. *Journal of Geology*, 102(5):539~558.
- Evans R J, Ashwal L D, Hamilton M A. 1999. Mafic, ultramafic, and anorthositic rocks of the Tete Complex, Mozambique: petrology, age, and significance. *South African Journal of Geology*, 102:153~166.
- Frimmel H E, Zartman R E, Spath A. 2001. The Rich tersveld Igneous Complex, South Africa: U-Pb zircon and geochemical evidence for the beginning of Neoproterozoic continental break up. *Journal of Geology*, 109:493~508.
- Fu Li. 2019. Determination of manganese content in a sample of titanium ore in Mozambique by volumetric method. *Chemical technology and development*, 48(07):38~39 (in Chinese with English abstract).
- Ganzev A A, Sotskav Y P, Lyapunov S M. 1984. Geochemical specialization of ore-bearing solutions in relation to rare-earth element. *Geochemistry*, 20:160~164.
- Gazel E, Plank T, Forsyth D W, Bendersky C, Lee C T A, Hauri E H. 2012. Lithosphere versus asthenosphere mantle sources at the Big Pine Volcanic Field, California. *Geochemistry, Geophysics, Geosystems*, 13(6):1~25.
- Goscombe B, Armstrong R, Barton J M. 2000. Geology of the Chewore Inliers, Zimbabwe: constraining the Mesoproterozoic to Palaeozoic evolution of the Zambezi belt. *Journal of African Earth Sciences*, 30:589~627.
- Grantham G H, Maboko M, Eglinton B M. 2003. A review of the evolution of the Mozambique Belt and implications for the amalgamation and dispersal of Rodinia and Gondwana. In: Yoshida M, Windley B F, Dasgupta S. (eds) *Proterozoic East Gondwana: Supercontinent Assembly and Breakup*. Geological Society, London, Special Publications, 206:401~425.
- Gray D R, Foster D A, Meert J G, Goscombe B D, Armstrong R, Trouw R A J, Passchier C W. 2008. A Damara Orogen perspective on the assembly of southwestern Gondwana. *Geological Society*, 294:257~278.
- Gu Alei, Wang Jie, Ren Junping, Zuo Libo, Sun Hongwei, Xing Shi, Liu Zijiang, Ezekiah Chikambwe. 2020. Geological characteristics and mineralization potential analysis for the Pan-African Hook Batholith in Central Zambia. *Geological Survey and Research*, 43(01):63~71+80 (in Chinese with English abstract).
- Hanson G N. 1980. Rare earth elements in the Petrogenetic Studies of igneous system. *Annual Review of Earth and Planetary Sciences*, 8:371~406.
- Hanson R E, Martin M W, Bowring S A, Munyanyiwa H. 1998. U-Pb zircon age for the Umkondo dolerites, eastern Zimbabwe: 1.1 Ga large igneous province in southern Africa/East Antarctica and possible Rodinia correlations. *Geology*, 26:1143~1146.
- Handke M J, Tucker R D, Ashwal L D. 1999. Neoproterozoic continental arc magmatism in west-central Madagascar. *Geology*, 27:351~354.
- Hanson R E. 2003. Proterozoic geochronology and tectonic evolution of southern Africa. *Geological Society London Special Publications*, 206:427~463.
- Haslam H W, Brewer M S, Darbyshire D P F, Davis A E. 1983. Irumide and post-Mozambique an plutonism in Malawi. *Geological Magazine*, 120:21~35.
- Hauzenberger C A, Bauernhofer A H, Hoinkes G, Wallbrecher E, Mathu E M. 2004. Pan-African high pressure granulites from SE-Kenya: Petrological and geothermobarometric evidence for a polycyclic evolution in the Mozambique belt. *Journal of*

- African Earth Sciences, 40:245~268.
- Hauzenberger C A, Sommer H, Fritz H, Bauernhofer A, Kröner A, Hoinkes G, Wallbrecher E, Thöni M. 2007. SHRIMP U-Pb zircon and Sm-Nd garnet ages from the granulitefacies basement of SE Kenya: evidence for Neoproterozoic polycyclic assembly of the Mozambique Belt. *Journal of the Geological Society*, 164(1):189~201.
- He Heling, Zhou Hang. 2012. Geological characteristics and genesis of ilmenite in Tete Province, Mozambique. *Industrial Technology*, 21(02):8~9 (in Chinese without English abstract).
- Hu Shiling, Wang Songshan, Sang Haiqing, Qiu Ji, Ye Donghu, Cui Renhe, Qi Changmou. 1990. Isotopic geological age, rare earth geochemistry and geological significance of Damiao anagite. *Geoscience*, (04):332~343 (in Chinese with English abstract).
- Hu Zhaochu, Gao Shan, Liu Yongsheng, Hu Shenghong, Chen Haihong, Yuan Honglin. 2008. Signal enhancement in laser ablation ICP-MS by addition of nitrogen in the central channel gas. *Journal of Analytical Atomic Spectrometry*, 23:1093~1101.
- Huang Jianping, Ye Shuiquan, Xia Mingfei. 2005. Types and geological characteristics of gold deposits in Mozambique. *Geology of Jiangsu province*, 29(1):4~27 (in Chinese with English abstract).
- Jamal D L, Zartman R E, Dewit M J. 1999. U-Pb single zircon dates from the Lurio belt, northern Mozambique; Kibaran and Pan-African orogenic events highlighted. *Journal of African Earth Sciences, Special Abstracts Issue, GSA 11: Earth Resources for Africa*, 28~32.
- Jacobs J, Fanning C M, Henjes-Kunst F, Olesch M, Paech H J. 1998. Continuation of the Mozambique Belt into East Antarctica: Grenville-age metamorphism and polyphase Pan-African high-grade events in central Dronning Maud Land. *J. Geol.*, 106:385~406.
- Jacobs J, Pisarevsky S, Thomas R J, Becker T. 2008. The Kalahari Craton during the assembly and dispersal of Rodinia. *Precambrian Research*, 160(1):142~158.
- Jean Chorowicz. 2005. The East African rift system. *Journal of African Earth Sciences*, 43:379~410.
- Johnson S P, Cutten H N C, Muhongo S, De Waele B. 2003. Neoarchaean magmatism and metamorphism of the western granulites in the central domain of the Mozambique belt, Tanzania: U-Pb SHRIMP geochronology and P-T estimates. *Tectonophysics*, 375:125~145.
- Johnson S P, Rivers T, De Waele B. 2005. A review of the Mesoproterozoic to early Palaeozoic magmatic and tectonothermal history of south-central Africa: implications for Rodinia and Gondwana. *Journal of the Geological Society, London*, 161:433~450.
- Johnson S P, De Waele B, Liyungu K A. 2006. U-Pb sensitive high-resolution on microprobe (SHRIMP) zircon geochronology of granitoid rocks in eastern Zambia: Terrane subdivision of the Mesoproterozoic Southern Irumide Belt. *Tectonics*, 25:1~450.
- Johnson S P, De Waele B, Evans D, Banda W, Tembo F, Milton J A, Tani K. 2007. Geochronology of the Zambezi Supracrustal Sequence, southern Zambia: a record of Neoproterozoic divergent processes along the southern margin of the Congo Craton. *Journal of Geology*, 115:355~374.
- Kerr A, Walsh J A, Sparkes G W, Hinchey J G. 2013. Vanadium potential in Newfoundland and Labrador: a review and assessment. Newfoundland and Labrador Department of Natural Resources, *Geological Survey*, 13:137~165.
- Key R M, Liyungu A K, Njamu F M, Somwe V, Banda J, Mosley P N, Armstrong R A. 2001. The western arm of the Lufilian Arc in NW Zambia and its potential for copper mineralization. *Journal of African Earth Sciences*, 33:503~528.
- Kong Huilei, Li Jinchao, Li Yazhi, Jia Qunzi, Guo Xianzheng, Zhang Bin. 2018. Zircon U-Pb dating and Geochemistry of the Jiadang Olivine Gabbro in the eastern Section of East Kunlun, Qinghai Province and Their Geological Significance. *Acta Geologica Sinica*, 92(05):964~978 (in Chinese with English abstract).
- Kröner A, Hegner E, Collins A S, Windley B F, Brewer T S, Razakamanana T, Pidgeon R T. 2000. Age and magmatic history of the Antananarivo block, Central Madagascar, as derived from zircon geochronology and Nd isotopic systematics. *American Journal of Science*, 300:251~288.
- Kröner A. 2001. The Mozambique belt of East Africa and Madagascar: significance of zircon and Nd model ages for Rodinia and Gondwana supercontinent formation and dispersal. *South African Journal of Geology*, 105:151~168.
- Kröner A, Willne A P, Hegner E, Jaeckel P, Nemchin A. 2001. Single zircon ages, PT evolution and Nd isotopic systematics of high-grade gneisses in southern Malawi and their bearing on the evolution of the Mozambique belt in southeastern Africa. *Precambrian Research*, 109:257~291.
- Le Bas M J, Le Maitre R W A, Streckesisen B, Zanetin. 1986. A Chemical Classification Volcanic Rocks Based of The Total Alkali-Silica Diagram. *Journal of Petrology*, 27(3):745~750.
- Li Xingli, Hou Minli, Jian Weizi, Birger Rasmussen, Stephen Sheppard, Simon AWilde, Jie Meng. 2019. Role of fluids in Fe-Ti-P mineralization of the Proterozoic Damiao anorthosite complex, China: Insights from baddeleyite-zircon relationships in ore and altered anorthosite. *Ore Geology Reviews*, 115:1~35.
- Lindsley D H, Frost B R, Frost C D, Scoates J S. 2010. Petrology, geochemistry and structure of the Chugwater Anorthosite, Laramie Anorthosite Complex, Southeastern Wyoming. *Canadian Mineralogist*, 48(4):887~923.
- Liu Yongsheng, Hu Zhaochu, Zong Keqing, Gao Changgui, Gao Shan, Xujian, Chen Haihong. 2010. Reappraisal and refinement of zircon U-Pb isotope and trace element analyses by LA-ICP-MS. *Chinese Science Bulletin*, 55(15):1535~1546.
- Liu Xiaoyang, Wang Jie, Yu Jinjie, Xiu Quanye, Wang Liying, He Fuqing, Ren Junping. 2015. Geo-tectonic and distribution pattern of Mineral resources in central south Africa. *Contributions of Geology and Mineral Resources Research*, 30:001~012 (in Chinese with English abstract).
- Liu Xiaoyang, Wang Jie, Ren Junping, Gong Penghui, He Shengfei, He Fuqing. 2017. Age of granites from the Chambishi copper mine in Zambia and its implications. *Geology in China*, 44(4):755~765 (in Chinese with English abstract).
- Ludwig K R. 2003. A Geochronological Toolkit for Microsoft Excel. Berkeley Geochronology Center California, Berkeley, 39 pp.
- Macey P H, Thomas R J, Grantham G H, Ingram B A, Jacobs J, Armstrong R A, Roberts M P, Bingen B, Hollick L, de Kock G S, Viola G, Bauer W, Gonzales E, Bjerkgård T, Henderson I H C, Sandstad J S, Cronwright M S, Harley S, Solli A, Nordgulen Ø, Motuza G, Daudi E, Manhica V. 2010. Mesoproterozoic geology of the Nampula Block, northern Mozambique: tracing fragments of Mesoproterozoic crust in the heart of Gondwana. *Precambrian Research*, 182:124~148.
- Marco A G. 1984. Petrochemistry, tectonic evolution and metasomatic mineralizations of Mozambique belt granulites from S Malawi and Tete (Mozambique). *Elsevier*, 25:161~186.
- Maboko M A H. 1995. Neodymium isotopic constraints on the protolith ages of rocks involved in Pan-African tectonism in the Mozambique Belt of Tanzania. 458 R. E. Hanson *Journal of the Geological Society, London*, 152:911~916.
- Meert J G. 2003. A synopsis of events related to the assembly of eastern Gondwana. *Tectonophysics*, 362:1~40.
- Middlemost E A K. 1985. *Magmas and Magmatic Rocks*. London: Longman, 1~266.
- Orozco-Esquivel T, Petrone C M, Ferrari L, Tagami T, Manetti P. 2007. Geochemical and isotopic variability in lavas from the eastern Trans-Mexican Volcanic Belt: Slab detachment in a

- subduction zone with varying dip. *Lithos*, 93(1-2):149~174.
- Peccerillo R, Taylor S R. 1976. Geochemistry of Eocene calcalkaline volcanic rocks from the Kastamonu area, northern Turkey. *Contributions to Mineralogy and Petrology*, 58:63~81.
- Pinna P, Jourde G, Calvez J Y, Mroz J P, Marques J M. 1993. The Mozambique Belt in northern Mozambique: Neoproterozoic (1100 ~ 850Ma) crustal growth and tectogenesis, and superimposed Pan-African (800 ~ 550Ma) tectonism. *Precambrian Research*, 62:1~59.
- Ren Junping, Wang Jie, ZuoLibo, Gu Alei, Sun Hongwei, Xu Kangkang, Chipilauka Mukofu, Alphet Phaskanido kowe, Ezekoah Chikambwe, Chishimba Canisius, Daniel Malunga. 2019. Zircon U-Pb geochronology, Lu-Hf isotopic compositions and geochemical characteristics of the quartzdiorites from western Kasamain northern Zambia. *Acta Geologica Sinica*, 93(11):2832~2846 (in Chinese with English abstract).
- Sacchi R, Cadoppi P, Costa M. 2000. Pan-African reactivation of the Lurio segment of the Kibaran Beltsystem; a reappraisal from recent age determinations in northern Mozambique. *Journal of African Earth Sciences*, 30:629~639.
- Schaerer U, Wilmart E, Duchesne J C. 1996. The short duration and anorogenic character of anorthositic magmatism; U-Pb dating of the Rogaland complex, Norway. *Earth Planet Sci Lett*, 139:335~350.
- Shinjo R, Chung S L, Kato Y. 1999. Geochemical and Sr-Nd isotopic characteristics of volcanic rocks from the Okinawa Trough and Ryukyu Arc: Implications for the evolution of a young, intracontinental back arc basin. *J. Geophys. Res.*, 104(B5):10591~10608.
- Sklyarov E V, Gladkochub D P, Mazukabzov A M, Menshagin Yu V, Watanabe T, Pisarevsky S A. 2003. Neoproterozoic mafic dike swarms of the Sharyzhgalskiy metamorphic massif, southern Siberian craton. *Precambrian Research*, 122(1):359~376.
- Stern R J. 1994. Arc assembly and continental collision in the Neoproterozoic East African Orogen: implications for the consolidation of Gondwana land. *Annual Reviews Earth and Planetary Sciences*, 22:319~351.
- Sun Jiming, Bai Jianke, Zhu Xiaohui, Ma Zhongping. 2018. Geochemistry of the Qijiaojing Formation Pillow Basalt in the Eastern Bogda Orogenic Belt, East Tianshan and Its Implications for Tectonic Setting. *Acta Geologica Sinica*, 92(03):520~530 (in Chinese with English abstract).
- Sun S S, Mcdonough W F. 1989. Chemical and isotopic systematics of oceanic basalts. Implications for mantle composition and processes. In: Saunders A D, Norry M J eds. *Magmatism in the Ocean Basins*. Geol. Soc. Spec. Pub., London, 42:313~345.
- Tucker R D, Ashwal L D, Handke M J, Hamilton M A, Le Grange M, Rambeloson R A. 1999. U-Pb geochronology and isotope geochemistry of the Archean and Proterozoic rocks of north-central Madagascar. *The Journal of Geology*, 107:135~153.
- Wang Yunliang, Zhang Chengjiang, Xiu Shuzhi. 2001. Th/Hf-Ta/Hf identification of tectonic setting of basalts. *Acta Petrologica Sinica*, 17(03):413~421 (in Chinese with English abstract).
- West D P, Coish R A, Tomascak P B. 2004. Tectonic setting and regional correlation of Ordovician metavolcanic rocks of the Casco Bay Group, Maine: Evidence from trace element and isotope geochemistry. *Geological Magazine*, 141(2):125~140.
- Wilmart E, Demaiffe D, Ducjesme J C. 1989. Geochemical Constraints on the Genesis of the Tellnes Ilmenite Deposit, Southwest Norway. *Economic Geology*, 84:1047~1056.
- Wu Yuanbao, Zheng Yongfei. 2004. Genesis of zircon and its constraints on interpretation of U-Pb age. *Chinese Science Bulletin*, 49(16):1589~1604. (in Chinese without English abstract).
- Viola G, Henderson I H C, Bingen B, Thomas R J, Smethurst M A, De Azavedo S. 2008. Growth and collapse of a deeply eroded orogen: insights from structural, geophysical, and geochronological constraints on the Pan-African evolution of NE Mozambique. *Tectonics*, 27:(TC5009).
- Xiao Xiaolin, Feng Ye, Liu Gaofeng. 2014. Discovery of the ilmenite ore deposit and prospecting potential in Angonia area, Mozambique. *Mineral Exploration*, 5(06):920~926 (in Chinese with English abstract).
- Zhang Zhaochong. 2018. Genesis of Proterozoic Anorthosites and Associated Fe-Ti-V-P Ore Deposits. *Bulletin of Mineralogy, Petrology and Geochemistry*, 37(6):1047~1091.
- Zhang Lianfeng, Zhang Zengqi, Liu Pengrui. 2006. Geological characteristics and genesis of deposit of Deposit in Juxian Tianbao Ilditite. *Shandong Land and Resources*, 22(02):45~52 (in Chinese with English abstract).
- Zhang Jianwen, Liang Han, Zhang Hua, Liu Yang, Ma Chongzhen, Zhong Wenli. 2013. Study on comprehensive utilization of rutile in a coastal placer in Mozambique. (S1):169~172 (in Chinese with English abstract).
- Zhou Yonggang. 2019. Analysis of geological characteristics and prospecting prospects of the Majiayulmenite deposit in Ju County, Shandong Province. *Journal of Shandong University of Technology (Natural Science edition)*, 33(05):58~62.
- Ziegler P A, Cloetingh S. 2004. Dynamic processes controlling evolution of rifted basins. *Earth-Science Reviews*, 64(1-2):1~50.
- Zuo Libo, Ren Junping, Wang J, Gu Alei, Sun Hongwei, Xu Kangkang, Alphet Phaskanido Kowe, Ezekiah Chikambwe. 2020. Geochemical characteristics, Zircon U-Pb ages and Lu-Hf isotopic composition of granites in Bangweulu Block, Zambia. *Geological Survey and Research*, 43(01):30~41 (in Chinese with English abstract).

## 参 考 文 献

- 陈正乐, 陈柏林, 李厚民, 杜维河, 李立兴, 韩凤彬, 王永, 孙岳, 吴玉, 张文高. 2014. 河北承德大庙铁矿床地质构造特征与找矿预测. *地质学报*, 88(12):2339~2350.
- 邓宇涛, 杨瑞茹, 张钊, 韩志华, 李莉. 2017. 莫桑比克滨海重砂矿床地质特征. *中国煤炭地质*, 29(12):31~35.
- 贺和岭, 周航. 2012. 莫桑比克太特省钛铁矿地质特征及成因探讨. *工业技术*, 21(02):8.
- 黄建平, 叶水泉, 夏明飞. 2005. 莫桑比克金矿类型及地质特征. *江苏地质*, 29(1):24~27.
- 傅立. 2019. 容量法测定某莫桑比克钛矿样品中的锰含量. *化工技术与开发*, 48(07):38~39.
- 古阿雷, 王杰, 任军平, 左立波, 孙宏伟, 邢仕, 刘子江, Ezekiah Chikambwe. 2020. 赞比亚中部泛非期 Hook 岩基地质特征及成矿潜力分析. *地质调查与研究*, 43(01):63~71+80.
- 胡世玲, 王松山, 桑海清, 裘冀, 叶东虎, 崔人合, 戚长谋. 1990. 大庙斜长岩同位素地质年龄、稀土地球化学及其地质意义. *地质科学*, (04):332~343.
- 孔会磊, 李金超, 栗亚芝, 贾群子, 国显正, 张斌. 2018. 青海东昆仑东段加当橄辉岩长岩锆石 U-Pb 年代学、地球化学及地质意义. *地质学报*, 92(05):964~978.
- 刘晓阳, 王杰, 余金杰, 修群业, 王丽瑛, 贺福清, 任军平. 2015. 中南部非洲的地质构造演化与矿产分布规律. *地质找矿论丛*, 30:001~012.
- 刘晓阳, 王杰, 任军平, 龚鹏辉, 何胜飞, 贺福清. 2017. 赞比亚谦比西铜矿花岗岩年龄及其指示意义. *中国地质*, 44(4):755~765.
- 任军平, 王杰, 左立波, 古阿雷, 孙宏伟, 许康康, Chipilauka Mukofu, Alphet Phaskanidokowe, Ezekoah Chikambwe, Chishimba Canisius, Daniel Malunga. 2019. 赞比亚北部省卡萨马西部石英闪长岩锆石 U-Pb 和 Lu-Hf 同位素及地球化学特征. *地质学报*, 93(11):2832~2846.
- 孙吉明, 白建科, 朱小辉, 牛峥, 马中平. 2018. 东天山博格达造山带东段七角井组枕状玄武岩地球化学特征及构造背景探讨. *地质学报*, 92(03):520~530.
- 汪云亮, 张成江, 修淑芝. 2001. 玄武岩类形成的大地构造环境的 Th/Hf-Ta/Hf 图解判别. *岩石学报*, 17(03):413~421.

吴元保,郑永飞. 2004. 锆石成因矿物学研究及其对 U-Pb 年龄解释的制约. 科学通报, 49(16):1589~1604.

肖晓林,冯晔,刘高峰. 2014. 莫桑比克安岗尼亚地区钛铁矿床的发现及找矿潜力. 矿产勘查, 5(06):920~926.

张招崇. 2018. 元古宙斜长岩体及其 Fe-Ti-P 矿床的成因. 矿物岩石地球化学通报, 37(6):1047~1091.

张建文,梁汉,张华,刘洋,马崇振,钟文利. 2013. 莫桑比克某海滨砂矿中金红石选矿综合利用研究. 有色金属(选矿部分), (S1):169~172.

张连峰,张增奇,刘鹏瑞. 2006. 莒县天宝钛铁矿地质特征及矿床成因探讨. 山东国土资源, 22(02):45~52.

周永刚. 2019. 山东省莒县马家峪钛铁矿矿床地质特征及找矿远景分析. 山东理工大学学报(自然科学版), 33(05):58~62.

左立波,任军平,王杰,古阿雷,孙宏伟,许康康, Alphet Phaskani Dokowe, Ezekiah Chikambwe. 2020. 赞比亚班韦乌卢地块花岗岩地球化学特征、锆石 U-Pb 年龄及 Lu-Hf 同位素组成. 地质调查与研究, 43(01):30~41.

## Zircon U-Pb age, geochemical characteristics and mineralization, geotectonic significance for anorthosite of the ilmenite field in Tete Province, Mozambique

LIU Gaofeng<sup>1)</sup>, LOU Fasheng<sup>\*1)</sup>, LUO Chunlin<sup>1)</sup>, WANG Bin<sup>1)</sup>, LIAO Liugen<sup>1)</sup>, LU Xianfeng<sup>1)</sup>, CHEN Haopeng<sup>1)</sup>, ZHU Changjie<sup>1)</sup>, CUMBANE Antonio<sup>2)</sup>, LIU Yongxu<sup>3)</sup>

1) *Geological Survey Institute of Jiangxi Province, Nanchang, 330030, China;*

2) *Matola Bureau of Geology, Mineral Resources and Energy, Matola, 1115, Mozambique;*

3) *Coalfield Geological Research Institute of Jiangxi Province, Nanchang, 330030, China*

*\* Corresponding author: oasiskobe@163.com*

### Abstract

Mozambique is located in southern Africa. It is rich in mineral resources, and is one of the major export countries of titanium ore. Currently most industrial mining is based on the titanium zirconium sand ore along the coast. The primary ilmenite deposits are far less explored, and their geological background is largely unclear. A series of anorthosite samples closely related to the primary ilmenite have been collected in the Tete Province, Mozambique. Zircon U-Pb ages for the anorthosite samples are  $580 \pm 5$  Ma, which indicate the time of rock formation. The chemical characteristics of the samples indicate that the anorthosites are low Ti, low Mg and low K tholeiites. Rare earth elements show obvious accumulation of plagioclase,  $\delta\text{Eu}$  shows extremely high positive anomaly; the LREE/HREE ratios are 8.27~21.44, which shows the enrichment of LREE, indicating that the anorthosites were formed by high-degree melting and crystallization differentiation of the primary mantle. The trace elements have obvious enrichment of Sr, Ba and other large-ion lithophile elements, as well as depletion of Zr, Nb and other high field strength elements. The Ta/Hf ratios are 0.1~0.26, Th/Ta ratios are 3.14~13.59, reflecting the formation of anorthosites in the continental retro-arc extensional tectonic environment. The study of the country rock of the ore-forming ilmenite has revealed that the genetic type of the ilmenite is late-stage magmatic crystallization differentiation, and the ore-forming model is crystallization, differentiation, pressure, filtration. Our data also show the important evidence of the 660~610 Ma Pan-African orogeny in the Zambezi tectonic zone in Mozambique.

**Key words:** Tete Province in Mozambique; ilmenite; anorthosite; mineralization; geotectonic significance